

An advanced single-particle model for C_3S hydration - validating the statistical independence of model parameters

Joseph J. Biernacki* and Manohar Gottapu

Department of Chemical Engineering, Tennessee Technological University, Cookeville, Tennessee, USA

(Received November 6, 2014, Revised April 7, 2015, Accepted April 20, 2015)

Abstract. An advanced continuum-based multi-physical single particle model was recently introduced for the hydration of tricalcium silicate (C_3S). In this model, the dissolution and the precipitation events are modeled as two different yet simultaneous chemical reactions. Product precipitation involves a nucleation and growth mechanism wherein nucleation is assumed to happen only at the surface of the unreacted core and product growth is characterized via a two-step densification mechanism having rapid growth of a low density initial product followed by slow densification. Although this modeling strategy has been shown to nicely mimic all stages of C_3S hydration – dissolution, dormancy (induction), the onset of rapid hydration, the transition to slow hydration and prolonged reaction – the major criticism is that many adjustable parameters are required. If formulated correctly, however, the model parameters are shown here to be statistically independent and significant.

Keywords: precast modeling; parameter estimation; statistical confidence; hydration; cement

1. Introduction

Solid-fluid non-catalytic reactions often involve simultaneous transport processes including diffusion and convection with concomitant physical and chemical changes including phase transformations, dissociation, dissolution, and precipitation. Frequently, such processes are treated as having a single rate limiting step i.e. the slowest process in the sequence. In reality, experimental observations, in this case for the hydration of tricalcium silicate (C_3S), have complex features involving more than one rate controlling mechanism and/or changing mechanisms with time and extent of reaction. Hence, a thorough consideration of the process chemistry, thermodynamics and transport processes, consistent with experimental mechanistic observations, are essential when modeling such coupled reactive-transport systems.

Kinetic processes such as phase transformation, crystallization, decomposition, and hydration are some of the example systems where the role of multiple rate controlling mechanisms and or transition between mechanisms can be significant. Many solid-fluid reactions typically show some or all of the following reaction rate transitions for isothermal conditions: (I) rapid dissolution, (II)

*Corresponding author, Professor, E-mail: jbiernacki@tntech.edu

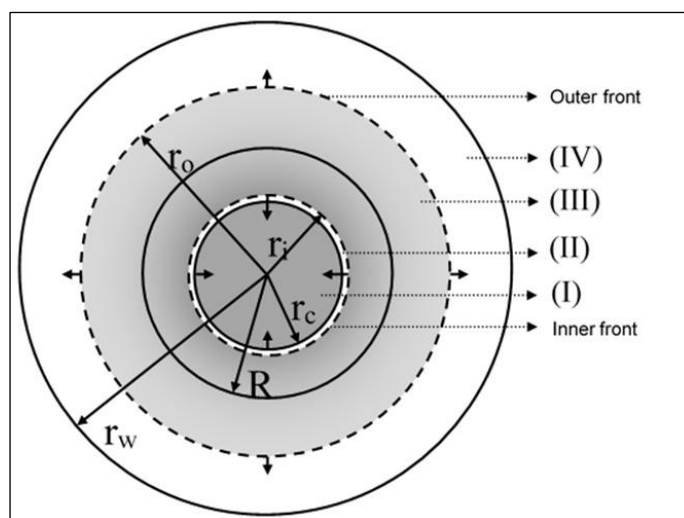


Fig. 1 Schematic diagram of a modified shrinking core model with densifying product layer (I: unreacted core (solid reactant), II: inner solvent layer, III: outer layer (solid product), and IV: outer solvent layer (aqueous phase); r_c , r_i , R , r_o , r_w : radii of unreacted reactant core, product inner front, original particle, product outer front, and finite aqueous layer respectively)

induction (no or very low reaction period), (III) acceleration (rapid increase in reaction rate), (IV) deceleration (rapid decrease in reaction rate), and (V) steady state (slow prolonged reaction) periods. Very large-scale industrial examples of such include hydration of calcium silicates (tricalcium silicate and dicalcium silicate) and calcium aluminates (tricalcium aluminate and calcium aluminosulfate), relevant in portland cement concrete (the world's most used material) and related cementitious materials widely used in construction and calcium sulfate hemihydrate, relevant in production of gypsum-based cements, wall board and other high volume construction products. In an effort to address the complexity of such processes, Biernacki and Xie (2011) introduced an "advanced single particle model (ASPM)" wherein they considered reactant dissolution, product nucleation at the unreacted core surface, transport of solution phase intermediates through a product layer, a shrinking unreacted core, an expanding outer product layer, and densification within the product layer. Inspired by the work of Pommersheim (1985), the complexity of the ASPM, unfortunately, requires the introduction of numerous adjustable parameters for which, at this time, known values are not available. In their prior work, a systematic strategy for estimation of model parameters is illustrated. The present study deals only with a statistical analysis to assess the interdependence of extracted model parameters.

2. Model definition/statement

A schematic diagram of the physical characteristics of the advanced single particle model is shown in Fig. 1. This figure illustrates the dissolution of a solid spherical reactant into a liquid solvent and the simultaneous precipitation of a porous solid product around the unreacted core. A thin solvent layer is assumed to always be in contact with the reacting particle. This thin inner liquid layer (Region (II) in Fig. 1) is the demarcation between the unreacted core and the

inner-most surface of the product layer. Due to this assumption, product nuclei are allowed to form and grow over time on the inner-most product surface instead of directly on the unreacted core surface. As the reactant core shrinks towards its center, the solid product layer (labeled as outer layer (III) in Fig. 1) grows both inward and outward. Furthermore, the product is assumed to form in two-steps, first filling the available space with a low bulk density proto-product and then densifying as the dissolution process progresses. This two-step densification mechanism is consistent with some experimental observations for hydration of tricalcium silicates which suggest that after nucleation, the hydrate product quickly grows at a fast primary densification rate and occupies the available space and then slowly densifies with a secondary rate. A finite available space is considered for product growth to limit the extent of reaction by employing a representative confinement volume. This representative volume averages the neighboring particle proximities and limits the product growth due to particle-particle occlusion. The volume available is proportional to the amount of solvent present and, in this model, is defined using the mass ratio of the liquid solvent and solid reactant (L/S). If chosen correctly, the resulting single particle behavior was shown to resemble that of an average particle in a random Avramian ensemble (Biernacki and Xie 2011).

A reaction mechanism (schema) is proposed in Fig. 2 for tricalcium silicate (C_3S)[†] hydration. As shown in Fig. 2, for C_3S hydration, the solid reactant core dissolves into the solvent (H_2O) and releases intermediates (Ca^{+2} , OH^- , $H_2SiO_4^{-2}$) which eventually precipitate as solid calcium silicate hydrate (C-S-H) product by reacting with additional water(solvent). The balance of these ions moves away from the core surface, through the product layer, and into the bulk solution where they react to precipitate as a solid by-product, calcium hydroxide (CH). The transport of $H_2SiO_4^{-2}$ ions is relatively slow when compared with that of Ca^{+2} and OH^- and hence single ionic (only $H_2SiO_4^{-2}$) transport and first order irreversible reaction kinetics is considered in this model. The validity of such an assumption is questionable, however, addition of the other ions is irrelevant for illustrative purposes here. Similarly, byproduct precipitation in the aqueous phase is neglected.

In summary, this complex shrinking core process consists of multiple simultaneous reactions including dissolution at the reactant surface, precipitation at inner and outer boundaries, product nucleation at the inner-most product surface, and a two-step densification mechanism within the product layer along with ionic transport through the product layer.

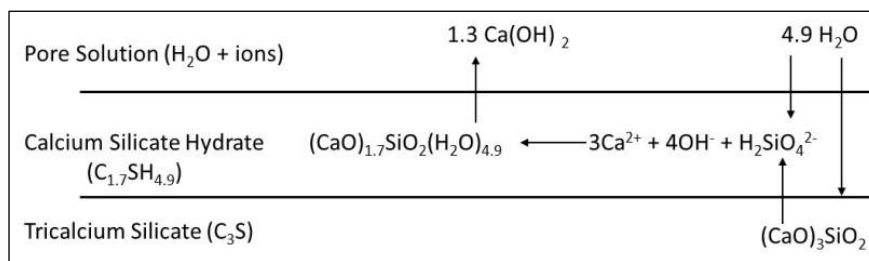


Fig. 2 Reaction schema diagram showing multiple reaction steps for the hydration of tricalcium silicate(C_3S)

[†]Cement chemists often uses a shorthand notation to represent cementitious oxides as follows: “CaO” is simply denoted as “C”. Similarly, SiO_2-S ; Al_2O_3-A ; Fe_2O_3-F ; $MgO-M$; K_2O-K ; Na_2O-Na ; SO_3-S ; CO_2-C ; H_2O-H ; Hence, tricalcium silicate ($(CaO)_3 \cdot SiO_2$) is written as C_3S in shorthand notation.

Table 1 Summary of key model assumptions

Solid C ₃ S core is non-porous
Spherical symmetry
No convective/bulk transport
First order rate laws
Product growth by heterogeneous nucleation and a two-step densification mechanism with two different rates: fast primary and low secondary

3. Governing equations

The model equations were derived using macroscopic and microscopic mass continuity formalisms

Macroscopic Mass Continuity

$$\frac{d}{dt} \int_{V_j} \rho_j dV_j = \oint_{A_j} (\vec{v}_j \rho_j \cdot \vec{n}) dA_j + \int_{V_j} R_j dV_j \quad (1)$$

where ρ_j , V_j , and A_j are the density, volume, and surface area of component j respectively, \vec{v}_j is the species velocity due to transport (diffusive and/or convective), and \vec{n} is the unit normal vector to the surface A . In the above equation, the first term on the right hand side is the transport flux term. Depending on the physics of system, the transport flux can be a diffusive, convective, reactive or a combined form. The second term is the source or the sink (i.e. the bulk reaction) term. The left hand term describes the time rate of change of mass of j within the control volume V .

Microscopic Mass Continuity

$$\frac{\partial c_j}{\partial t} = \vec{\nabla} \cdot D_j \vec{\nabla} C_j - \vec{\nabla} \cdot \vec{v} C_j + R_j \quad (2)$$

where \vec{v} is the convective velocity, C , D , and R are concentration, diffusion coefficient, and bulk reaction terms respectively for species j . Similarly, in the above equation, the first two terms on the right hand side are diffusive and convective fluxes and the third is the homogeneous reaction term. The left hand term is the time rate of change of concentration of species j .

Notable features of this model include the incorporation of surface nucleation. Biernacki and Xie (2011) describe the model in some detail, however, for clarity, the following two empirical equations that govern nucleation are provided here in brief

$$\frac{dN}{dt} = K_N s (C_i - C_p^{eq}) \quad (3)$$

$$\frac{ds}{dt} = -K_S s N (C_i - C_p^{eq}) \quad (4)$$

where N is the number of product nuclei, s is the active surface area available for new nuclei formation, K_N , K_S are the nucleation and surface area coverage rate constants. Since nucleation is happening only at the inner product front, the respective ionic concentration (C_i) is used in the above first order kinetic equations, where the subscript “ i ” indicates at the inner product surface.

Similarly, the model for product growth and densification is unique and is given here for clarity

$$\frac{\partial \rho}{\partial t} = \begin{cases} \text{if } \rho < \rho_p & K_D \rho (\rho_p - \rho) (C_j - C_p^{eq}) + K_{Ds} \rho (\rho_s - \rho) (C_j - C_p^{eq}) \\ \text{if } \rho > \rho_p & K_{Ds} \rho (\rho_s - \rho) (C_j - C_p^{eq}) \end{cases} \quad (5)$$

where K_D , K_{Ds} are the primary and secondary densification rate constants describing the two-step mechanism, ρ is the density of the product at any given point in the outer product layer, ρ_p and ρ_s are the maximum attainable primary and secondary densities of the product, and C_p^{eq} is the equilibrium solubility of the product. Note that the product layer co-densifies initially with both primary and secondary rates, however, once the primary density is achieved i.e. when the primary product fills the entire available space, further densification can only occur via the secondary densification rate.

Tables 1 through 4 summarize all model equations and parameters. Additional details can be found in Biernacki and Xie (2011).

In a prior work of the senior author, the ASPM was systematically parameterized to illustrate various combined rate controlling processes and a set of nominal, non-optimized parameters were established without statistical analysis (Biernacki and Xie 2011). The present study endeavors to establish the statistical relationship between kinetic rate parameters and the level of statistical confidence that one might expect if such a model is used to extract an optimal parameter set.

4. Results and discussion

As a starting point for the present study, the model was tuned so that it would mimic isothermal tricalcium silicate hydration; a typical hydration calorimetry curve, heat flow versus time, was used. The reference experimental data used was for an aqueous suspension of C₃S with a median particle diameter of 5 μm prepared with a water/cement (i.e. w/c) mass ratio of 0.4 and reacted at a constant temperature of 25°C. The obtained calorimetry heat curve was normalized by the sample initial mass, refer to Fig. 3. Note that Fig. 3 is plotted omitting the rapid dissolution peak and that the induction period is very short for this particular sample of C₃S. Although the rapid dissolution peak is not shown, the model is nonetheless able to mimic the induction stage accurately.

The baseline model fixes as many parameters as possible and as reasonable. Table 3 summarizes the fixed parameters. Raw material properties, density and molecular weights, are known quantities. The density of C-S-H (2.2 g/cc) as well as the molecular weight (243.6 g/mole[‡]) are within the range of accepted values. The density of the primary C-S-H is taken to be consistent with both the observation that the onset of Stage V hydration occurs at a total mass conversion of about 30% (Thomas 2007) and values previously suggested by Bishnoi and Scrivener (2009). The diffusivity of H₂SiO₄⁻² can be reliably estimated from correlations and the equilibrium concentrations computed from known thermodynamic data. Finally, the initial surface fraction available for nucleation is clearly unknown, but should be fixed for purposes of this work at some value near, but not equal to 1, to provide some small amount of pre-existing nuclei to seed growth. With the fixed parameters defined, only the reaction rate parameters, those parameters that are most difficult to estimate by other means, remain as fit parameters. Table 4 summarizes the nominal (baseline starting point) kinetic parameter set along with optimal values and their respective standard errors and p-values. Optimization and statistical analysis was performed using

[‡] The molecular weight of C-S-H was calculated for an assumed empirical formula of C_{1.7}SH_{4.9}.

MatLab's "nlinfit" package.

Standard errors were found to be reasonable in all cases, nominally 10% or less (in most cases much less) of the parameter value and p-statistics were all below 0.05 (in most cases much below

Table 2 Final equation system of multi-physical single particle model (shown in Lagrangian frame of reference coordinates and in dimensional form)

<u>Ionic Transport:</u>		<u>Pore Solution Balance:</u>	
Governing Equation		$V_o \frac{dC_o}{dt} = -4\pi r_o^2 [K_o(C_o - C_p^{eq})f_o + D_s \frac{dC_o}{dr_o}]$ (Eq. 2.6)	
$\frac{dC_j}{dt} - \frac{dr}{dt} \cdot \frac{\partial C_j}{\partial r} = \frac{1}{r^2} \frac{\partial}{\partial r} (Dr^2 \frac{\partial C_j}{\partial r}) + \frac{1}{w_p} \frac{dp}{dt}$ (Eq. 2.1)		$V_i \frac{dC_i}{dt} = 4\pi r_i^2 [K_i(C_i - C_p^{eq})f_i + D_s \frac{dC_i}{dr_i}]$ (Eq. 2.7)	
Boundary Conditions:		Where	
@ $r = r_i \rightarrow C_j = C_i$		$f_i = (1 - s_o)\rho_i$	
@ $r = r_o \rightarrow C_j = C_o$		$f_o = (1 - s)\rho_o$	
<u>Dissolution:</u>		<u>Nucleation:</u>	
$\frac{dr_c}{dt} = -K_d \vartheta_c (C_c^{eq} - C_i)$ (Eq. 2.2)		$\frac{dN}{dt} = K_N s (C_i - C_p^{eq})$ (Eq. 2.8)	
<u>Precipitation:</u>		<u>Surface Coverage:</u>	
$\frac{dr_i}{dt} = -K_i \vartheta_p (C_i - C_p^{eq})$ (Eq. 2.3)		$\frac{ds}{dt} = -K_s s N (C_i - C_p^{eq})$ (Eq. 2.9)	
$\frac{dr_o}{dt} = K_o \vartheta_o (C_o - C_p^{eq})$ (Eq. 2.4)			
<u>Two-step Densification:</u>			
$\frac{d\rho}{dt} - \frac{dr}{dt} \cdot \frac{\partial \rho}{\partial r} = \begin{cases} \text{if } \rho < \rho_p & K_D \rho (\rho_p - \rho) (C - C_p^{eq}) + K_{D_s} \rho (\rho_s - \rho) (C - C_p^{eq}) \\ \text{if } \rho > \rho_p & K_{D_s} \rho (\rho_s - \rho) (C - C_p^{eq}) \end{cases}$ (Eq. 2.5)			

Table 3 Material properties, fixed model parameters and physical constants for tricalcium silicate case study.

Parameter	Value	Units	Description
ρ_c	3.2	g/cm ³	Density of reactant (C ₃ S)
ρ_w	1	g/cm ³	Density of water
ρ_p	0.66	g/cm ³	Primary C-S-H product density
ρ_s	2.2	g/cm ³	Secondary C-S-H product density
$s\theta$	0.99	Initial surface fraction available for nucleation
D_s	0.0001	cm ² /sec	Diffusion coefficient of silicate ions (H ₂ SiO ₄ ⁻²)
c_c^c	0.00001	mole/cm ³	H ₂ SiO ₄ ⁻² concentration in equilibrium with C ₃ S
c_p^p	0	mole/cm ³	H ₂ SiO ₄ ⁻² concentration in equilibrium with C-S-H
w_c	228.3	g/g-mole	Molecular weight of C ₃ S
w_p	243.6	g/g-mole	Molecular weight of C-S-H

0.05) indicating that all model parameters are statistically significant at the greater than 95% confidence level.

Demonstrating mathematical independence, however, is somewhat more difficult. While, statistical confidence indicates that a parameter effects a change, it does not imply that one parameter is independent of another. To demonstrate independence, a series of additional optimization runs (experiments) were conducted in which a single parameter from the baseline parameter set was perturbed and the remaining six were varied until a new optima was achieved. The goodness of fit for the new optima was then compared to that for the baseline case. This procedure is suggested by Motulsky and Christopoulos (2004) wherein they state, "... if you change the value of one parameter and fix it, and then... find a new best-fit... when the parameters are completely unlinked... changing one parameter makes the fit worse, and you can't compensate at all by changing the other[s]. In this extreme case... the correlation... [is] zero... When two parameters are completely intertwined... changing one... makes the fit worse, but this can be completely compensated for by changing the other... the correlation... [is]... 1...". Fig. 4 compares the sum of squared errors that results when the procedure suggested by Motulsky and Christopoulos is systematically applied to each of the seven rate parameters. In every case, except for k_n and k_s , the sum of squared error is higher for the perturbed optimization than for the un-perturbed case. This demonstrates that parameters k_d , k_i , k_o , k_D and kD_s are largely independent, one from the other. In the case of k_n and k_s , however, it was found that indeed they are dependent and in fact are one-for-one inversely correlated, i.e. if k_n is increased by a factor of 10, then when k_s is decreased by 10, the same results are achieved. This is logical since both the rate of nucleation (k_n) and the rate of surface coverage (k_s) achieve the same outcome and have identical mathematical forms, refer to Table 2, Eqs. (2.3) and (2.4), i.e. they both produce reaction product that covers the surface of the particle. Therefore, with the present model formulation it is impossible to quantify, in an absolute sense, the magnitude of k_n and k_s one relative to the other by model fitting of the sort described here. Nonetheless, both k_n and k_s were found to be independent of the other five parameters.

To further support these finding, the correlation matrix was produced, refer to Table 5. The correlation matrix confirms that k_n and k_s are inversely correlated, the correlation parameter is -0.938 and that k_d , k_i , k_o , k_D and kD_s are largely uncorrelated though k_o and k_D show a weak correlation having a correlation parameter of -0.691. This is also logical since the rate at which product is formed will be related to the rate at which the produce front advances (k_o) and the rate at which that product densifies (kD).

Finally, parameters derived using the present formalism and those derived using other approaches must be compared and reconciled if possible. In an earlier work, Xie and Biernacki (2011) discussed at length the many models that have been used and developed for fitting tricalcium silicate hydration data. Among these are the equations of Jander, and Ginstling and Brounshtein (see Brown 1985, Taplin 1968, Pommersheim *et al* 1985), Avrami (see Brown *et al* 1985, Tennis and Jennings 2000), Cahn (see Thomas 2007, Bishnoi and Scrivener 2009)). In summary, approaches assuming that Stage II-V hydration is diffusion controlled (Brown 1985, Taplin 1968 and Pmmersheim 1985), have been largely rejected (Biernacki and Xie 2011, Xie and Biernacki 2011). Furthermore, the use of zero order reaction kinetics is pervasive throughout many of these modeling approaches (Tennis and Jennings 2000, Bishnoi and Scrivener 2009), an assumption that is clearly false (Juilland *et al.* 2010). Therefore, comparing the present results to model parameters that uses any of these formalisms is irrelevant. Finally, Bullard (2010) introduced a comprehensive modeling platform based on the application of kinetic cellular

automaton. His model, referred to as HydratiCA, includes separate dissolution, nucleation and precipitation reactions as well as transport effects and has been shown to reproduce Stage I, II and III features of C_3S hydration, although it is yet to adequately describe the Stage III-IV transition. The ASPM described here is an early attempt to assimilate features of HydratiCA using a continuum approach that promises to be computationally more efficient. The present model, however, utilizes first-order reaction kinetics in terms of a single ionic species ($H_2SiO_4^{-2}$) whereas HydratiCA assumes that all reactions are elementary as written, an assumption that is also unsupported experimentally at this point in time. And, while HydratiCA and the continuum-based model presented in this work are closely related, comparing model parameters extracted from experimental datasets would not be relevant because of the fundamentally different assumptions being made to describe the kinetic rate laws. The purpose, however, of such models, both the present continuum strategy and HydratiCA, are to provide computational platforms for testing various rate laws in hopes of eventually reconciling models and validating hypotheses for such complex processes such as tricalcium silicate hydration and the hydration of similar synthetic and naturally occurring minerals.

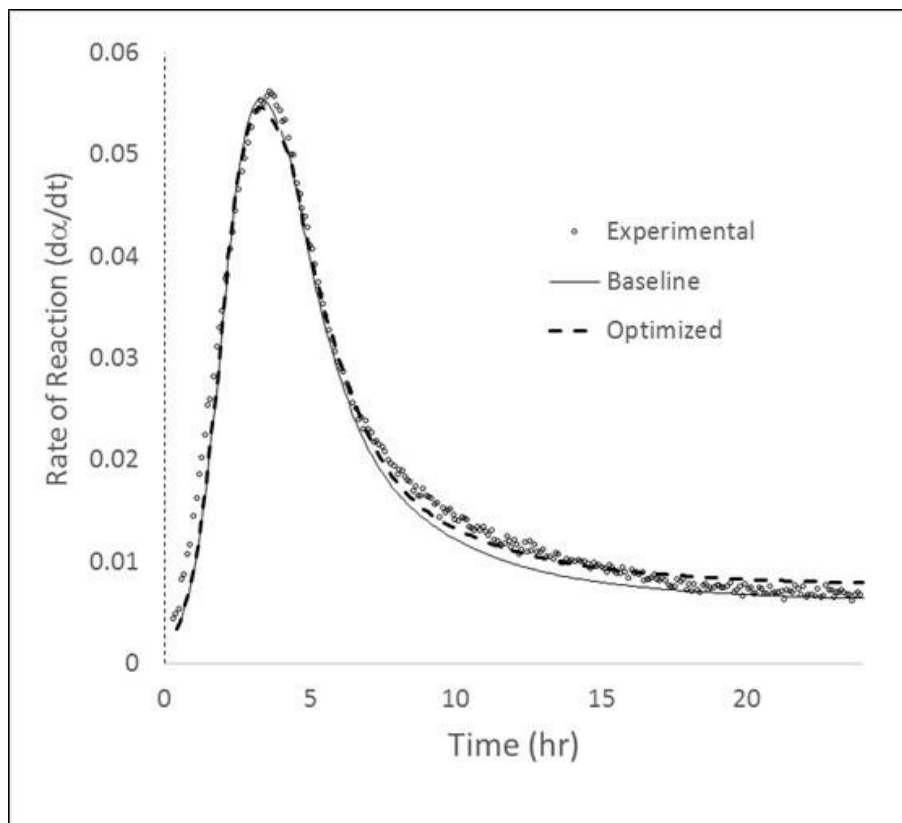


Fig. 3 Baseline case study illustrating the model prediction with the hypothesized two-step product growth process in an exponential representative volume confinement (experimental data is of tricalcium silicate hydration behavior for the first 25 hours of hydration time)

Table 4 Baseline parameter set for tricalcium silicate case study

Parameter	Value	Units	Description	Optimal Values	Standard Error	p-value
k_d	0.2	cm/hr	Dissolution rate constant	0.17	0.016	6.40E-22
k_i	3.33	cm/hr	Reaction rate constant at inner front	1.05	0.2	2.83E-07
k_o	0.047	cm/hr	Reaction rate constant at outer front	0.045	0.0013	3.03E-97
k_D	3.17×10^5	cm ³ /mol·hr	Nucleation rate constant	3.17×10^5	2.855×10^3	6.04E-211
kD_s	1.58×10^3	cm ³ /mol·hr	Surface coverage rate constant	2.13×10^3	9.05×10^1	1.32E-64
k_n	5×10^3	cm ⁶ /g ² ·hr	Primary densification rate constant	4.74×10^3	1.47×10^3	1.45E-03
k_s	1×10^5	cm ⁶ /g ² ·hr	Secondary densification rate constant	1.01×10^5	2.28×10^4	1.41E-05

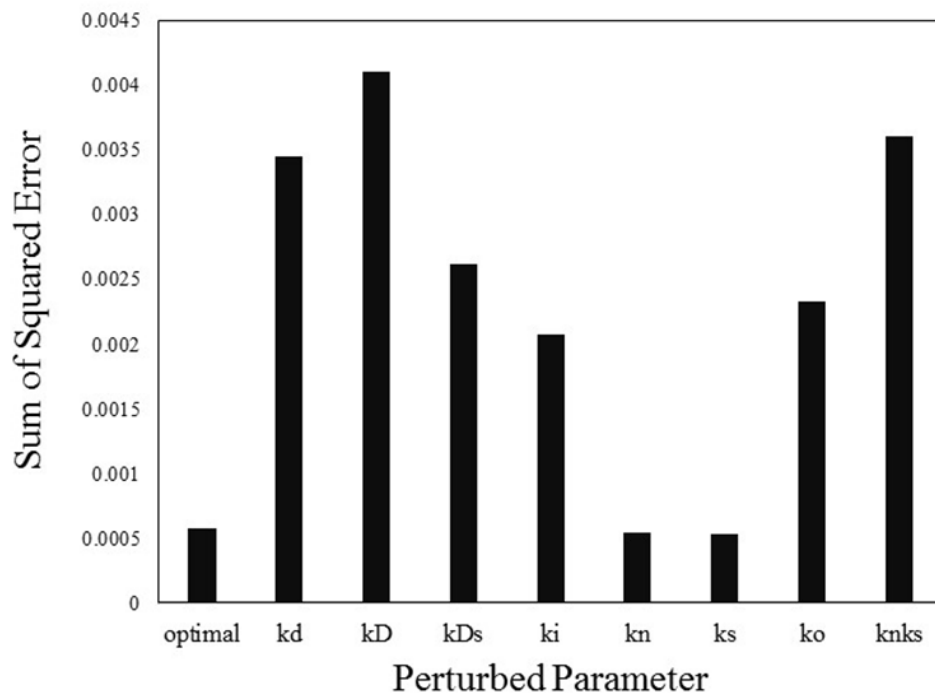


Fig. 4 Sum of squared error when each successive parameter, k_d , k_i , k_o , k_n , k_s , k_D and kD_s , was perturbed and then held constant and the optimization was run omitting that variable

Table 5 Correlation matrix for seven rate parameters

	kd	ki	ko	kD	kDs	ks	kn
kd	1.000	-0.340	-0.238	0.059	-0.014	0.144	-0.185
ki	-0.340	1.000	0.084	-0.191	-0.205	-0.226	0.291
ko	-0.238	0.084	1.000	-0.691	0.021	-0.096	-0.165
kD	0.059	-0.191	-0.691	1.000	0.031	0.105	0.085
kDs	-0.014	-0.205	0.021	0.031	1.000	0.025	-0.200
ks	0.144	-0.226	-0.096	0.105	0.025	1.000	-0.938
kn	-0.185	0.291	-0.165	0.085	-0.200	-0.938	1.000

5. Conclusions

A statistical analysis and optimization study was done to identify relationships between ASPM variables. Among the seven adjustable reaction rate parameters, only the nuclei formation and lateral growth rates were found to be co-variant, yet statistically independent of the other five rate constants. The high degree of statistical independence of the seven rate parameters, makes it possible to discern reaction effects even for this system of highly coupled events.

Apart from these findings, there are certain simplifications considered in this model which further need to be addressed. When applying this type of multi-parameter model, a complete set of experimental data is necessary for model verification and parameter estimation. For example, simple first order kinetic rate expressions based on a single intermediate ions were used in this model, however, an arbitrary kinetic rate expressions with a multi-ionic system may be required to determine the order of reactions and for correct model fitting. The role of by-product precipitation was completely ignored in this rather simplified model. By-product nucleation and growth kinetics might be relevant depending upon the application and can be a rate controlling factor. Hence, respective kinetic rate expressions for by-product precipitation need to be included for accurate model predictions. Initiation of the growth process using instantaneous nucleation was a simplification used to avoid the complexity of product nucleation. This approach is only valid when product nucleation is very fast or when nuclei are pre-existent and can be relaxed by triggering nucleation at the correct critical super-saturation, if known. Finally, this model is not intended to replace discrete-particle simulation environments. Yet, the single particle continuum-based modeling approach may be used to further develop hybrid strategies incorporating particle ensembles for microstructure development and in multi-scale simulations.

Acknowledgements

The authors would like to acknowledge partial financial support from the National Science Foundation under grant No. 0757284 and the Tennessee Tech University Center for Manufacturing research (CMR).

References

- Biernacki, J.J. and Xie, T. (2011), "An advanced single particle model for C_3S and alite hydration", *J. Am. Ceram. Soc.*, **94**(7), 2037-2047.
- Bishnoi S. and Scrivener, K. (2009), "Studying nucleation and growth kinetics of alite hydration using mic", *Cement. Concrete. Res.*, **39**(10), 849-860.
- Brown, P.W. (1985), "A kinetic model for the hydration of tricalcium silicate", *Cement. Concrete. Res.*, **15**(1), 35-41.
- Brown, P.W., Pommersheim, J.M. and Frohnsdorff, G. (1985), "A Kinetic Model for the Hydration of tricalcium silicate", *Cement. Concrete. Res.*, **15**(1), 35-41.
- Bullard, J.W. (2010), "New insights into the effect of calcium hydroxide precipitation on kinetics of tricalcium silicate hydration", *J. Am. Ceram. Soc.*, **93**(7), 1894-1903.
- Juilland, P., Gallucci, E., Flatt, R. and Scrivener, K. (2010), "Dissolution theory applied to the induction period in alite hydration", *Cement. Concrete. Res.*, **40**(6), 831-844.
- Motulsky, H. and Christopoulos, A. (2004), *Fiting Models to Biological Data Using Linear and Nonlinear Regression-A Practical Guide to Curve Fitting*, Oxford University Press, Oxford, UK.
- Pommersheim, J.M. (1985), "A kinetic model for the hydration of tricalcium silicate", *Cement. Concrete. Res.*, **15**(1), 35-41.
- Taplin, J. (1968), "On the hydration kinetics of hydraulic cements", *Proceedings of the 5th International Symposium on the Chemistry of Cement*, Tokyo.
- Tennis P.D. and Jennings H.J.M. (2000), "A model for two types of calcium silicate hydrate in the microstructure of portland cement pastes", *Cement. Concrete. Res.*, **30**(6), 855-863.
- Thomas, J. (2007), "A new approach to modeling the nucleation and growth kinetics of tricalcium silicate hydration", *J. Am. Ceram. Soc.*, **90**(1), 3282-3288.
- Xie T. and Biernacki, J.J. (2011), "The origins and evolution of cement hydration models", *Comput. Concr.*, **8**(6), 647-675.

CC